ACS APPLIED MATERIALS & INTERFACES

Letter

www.acsami.org

Preferentially Grown Ultranano c-Diamond and n-Diamond Grains on Silicon Nanoneedles from Energetic Species with Enhanced Field-Emission Properties

Joseph P. Thomas,*[,†,‡,§] Huang-Chin Chen,[†] Shih-Hao Tseng,[‡] Hung-Chi Wu,[‡] Chi-Young Lee,[‡] Hsiu Fung Cheng,[⊥] Nyan-Hwa Tai,[‡] and I-Nan Lin*[,†]

[†]Department of Physics, Tamkang University, Tamsui, Taiwan 251, R.O.C.

[‡]Department of Materials Science and Engineering, National Tsing-Hua University, Taiwan 300, R.O.C.

[⊥]Department of Physics, National Taiwan Normal University, Taiwan 116, R.O.C.

Supporting Information

ABSTRACT: The design and fabrication of well-defined nanostructures have great importance in nanoelectronics. Here we report the precise growth of sub-2 nm (c-diamond) and above 5 nm (n-diamond) size diamond grains from energetic species (chemical vapor deposition process) at low growth temperature of about 460 °C. We demonstrate that a pre-nucleation induced interface can be accounted for the growth of c-diamond or n-diamond grains on Si-nanoneedles (Si-NN). These preferentially grown allotropic forms of diamond on Si-NN have shown high electron field-emission properties and signify their high potential towards diamond-based electronic applications.

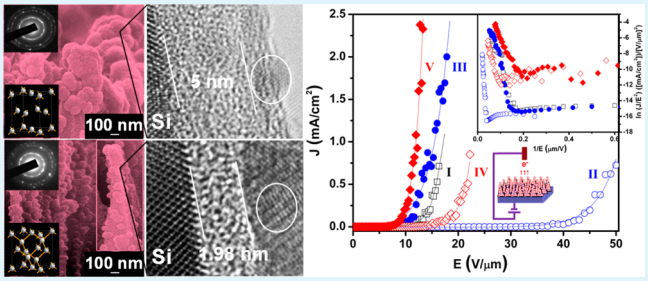

KEYWORDS: *c-diamond, n-diamond, silicon nanoneedles, chemical vapor deposition, electron field emission*

1. INTRODUCTION

Diamond has been gaining attention recently as an electronic material with its applications ranging from quantum computing to quantum-dot-based biomedical imaging, drug delivery, photonic and vacuum microelectronic devices, etc.[1−10] The invention of nano- or ultrananocrystalline diamond (UNCD), which preserves the unique physical or chemical properties of diamond and has abilities to improve heat removing and electronic properties of nanodevices, improved the scenario for their use in nanoelectronics.[6−18] Moreover, UNCD has also shown great potential for electron field-emitter applications.[6−10,13] For the advancement of nanodiamond-based nanoelectronics, the design, fabrication, and integration of well-defined nanostructures with optimized properties is required. To build diamond-based devices, a continuous, dense, and smooth diamond film on Si or other nondiamond substrates is decisive, which could be achieved only after an appropriate pre-nucleation technique prior to the growth process.[19−24] Furthermore, the nucleation process is essential to control the nanostructural growth as well as to engineer the material properties at the nanoscale. Different pre-nucleation techniques have already been explored to enhance the nucleation and growth of diamond on substrates.[19−29] Among the different pre-nucleation techniques, diamond nucleation using ultrasonication in a mixture of metal and nanodiamond particles has been found to be a simple, efficient, and reproducible method for planar substrates.[22−29] This process effectively create nucleation sites for the diamond growth from the cooperative effect of both metal and diamond particles during the ultrasonication process by inducing physico-chemical modification on the substrate surfaces.[22−30] However, these techniques have limitations for creating nucleation sites on nanostructures, because they can cause damage and even destroy the shape, sharpness, and properties of nanostructures.

The emerging trend in nanotechnology or nanoelectronics-based research is the exploration of new novel materials that could replace Si, where Si is serving as the back bone material for semiconductor industries for the past several years, or to integrate with Si nanostructures to obtain superior properties. Besides, enhancement in the electron field emission (EFE) and electronic properties of Si nanostructures have already been reported.[13,31−35] Considering the fact that the integration of nanostructured Si with UNCD could be an alternate choice for a better electronic nanomaterial, here we have chosen Si nanoneedles (Si-NN) as a model system to integrate with UNCD. Similar earlier efforts could grow UNCD on Si nanostructures;[13,33−35] but the nucleation and uniform growth have always been an issue. In addition, their growth behavior at

Received: August 11, 2012
Accepted: September 27, 2012
Published: September 27, 2012

the nanoscale has not been completely understood yet. In this work, a modified pre-nucleation process is envisioned to create nucleation sites and thereby achieve conformal UNCD growth while preserving their unique nanostructure features. We have found the formation of sub-2 nm c-diamond grains by using the modified pre-nucleation process, which is otherwise always found to grow n-diamond grains (allotropy of c-diamond) on Si substrates under the same growth conditions. The formation of these allotropic forms of diamond from energetic species is clearly distinguished for the first time and the mechanism of their growth at the nanoscale is proposed. Furthermore, their electron field-emission properties have been compared.

2. RESULTS AND DISCUSSION

Figure 1a shows typical FESEM image of pristine Si-NN (Si-NN_0) and inset shows TEM image of a Si-NN_0. The Si-NN_0 is about 4−5 μm in length and shows a very sharp apex. To create nucleation sites on Si-NN_0 prior to the growth of UNCD, the conventional pre-nucleation process is utilized first, in which the substrates are lying at the bottom of a beaker with Si-NN_0 faced up (see Figure S1 in the Supporting Information). Such an ultrasonication process is designated as UN_U process. The Si-NN obtained in such a manner is designated as Si-NN_1 and the UNCD coated Si-NN_1 is designated as UNCD/Si-NN_1 (Figure 1b). The FESEM image reveals that the UN_U process could significantly damage the nanoneedles, degraded the sharpness, and reduced the length of the needles to about few micrometers. The inset in Figure 1b shows a non-uniform UNCD growth and formation of large clusters of grains (size of 200−500 nm) on mostly at the tip of nanoneedles. The EFE property is enhanced after UNCD growth; however is significantly reduced because of the UN_U process, which will be discussed later. These results suggest the requirement of a new pre-nucleation process that can preserve the nanostructures intact during the process while efficiently creating nucleation sites and thereby further enhance the properties.

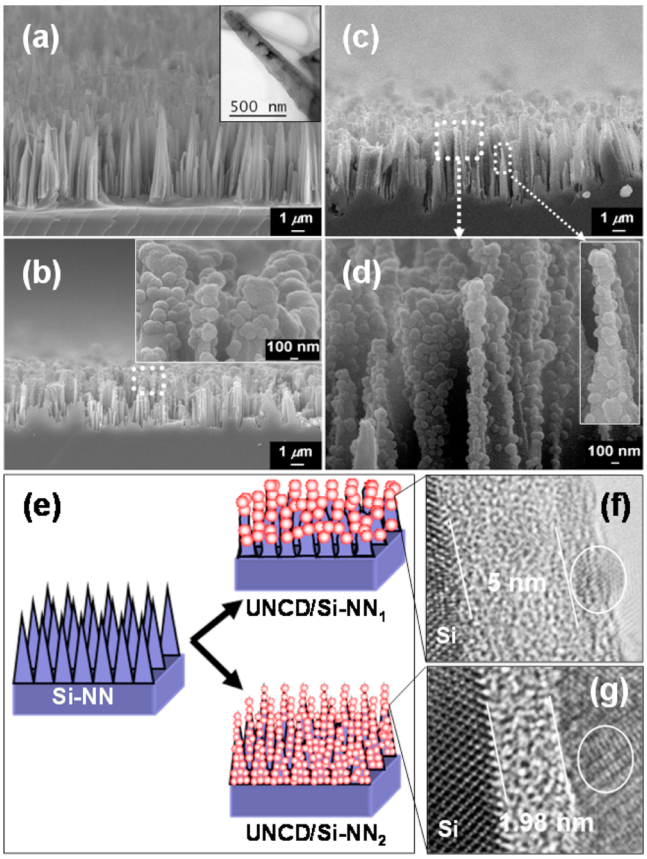

Figure 1. (a) FESEM image of as-prepared Si nanoneedles (Si-NN) and the inset shows TEM image of a tip, (b) FESEM image of UNCD grown Si-NN after the UN_U process (UNCD/Si-NN_1) with the inset showing the magnified image from selected area (dotted squares) of UNCD grown tip edges, (c) FESEM image of UNCD grown Si-NN after the UN_D process (UNCD/Si-NN_2), (d) high-magnification image of selected square areas from c shown with arrows, (e) schematics of the fabricated Si-NN before and after the UNCD growth and cross-sectional TEM images showing the interface between UNCD and Si for (f) UNCD/Si-NN_1 and (g) UNCD/Si-NN_2.

Prior to design a new pre-nucleation process, we have investigated in detail the materials and the mixed powder solution (Ti and nanodiamond in methanol solution), which has not yet been thoroughly studied previously to understand their effect in modifying the properties. Our studies show the Ti powder contain wide distribution of particles size, a few nanometers to tens of micrometers, and nanodiamond particles size are about 4−20 nm. A sample collected from the bottom of the mixed powder solution, which has been used for the nucleation processes, shows a mixture of mostly micrometer size Ti and nanodiamond powder particles (see Figure S2 in the Supporting Information). Whereas the sample collected from top of the solution contains only nano size Ti and nanodiamond particles (see Figure S2 in the Supporting Information). Although the fine and very light nanodiamond particles are expected to create little impact damage on Si-NN_0, the large titanium particles contain in the Ti powder are heavy and may cause large bombardment damage on Si-NN_0. Fortunately, the large Ti-particles usually sediment at the bottom of the solution and only the small Ti-particles can float on the upper portion of the container. Therefore, we designed a new ultrasonication process based on such a characteristic, viz., by keeping the substrate on top of the solution with the tips facing down, gently touching the solution, so that only small Ti and nanodiamond particles in the solution bombard on Si-NN_0 during the nucleation process, which is designated as UN_D process (see Figure S1 in the Supporting Information). The Si-NN_0 undergone the UN_D process and after the UNCD growth are designated here as Si-NN_2 and UNCD/Si-NN_2, respectively. It is interesting to note that the sharp apex of Si-NN_2 is preserved similar to the Si-NN_0 even after subjecting to the UN_D process and UNCD growth (Figure 1c, d). The inset in Figure 1d confirms the conformal growth of UNCD on Si-NN_2. The UNCD growth processes on Si-NNs are schematically depicted in Figure 1e. To clearly understand the effect of pre-nucleation processes on the UNCD growth, we have carried out cross-sectional TEM studies (Figure 1f, g) to investigate the interface between UNCD and Si and are discussed in the later part.

TEM studies have been carried out to obtain a detail insight into the UNCD growth on Si-NN_0. Figure 2a shows typical low magnification TEM image of a UNCD/Si-NN_2. This image again confirms the conformal growth of UNCD from the tip to bottom of Si-NN_2. To further investigate the growth properties, we have compared SAD patterns of pristine Si-NN, UNCD/Si-NN_1, and UNCD/Si-NN_2 (Figure 1b-d). The Si-NN SAD pattern indicates that the tips are [100] oriented. Typical (111), (220), and (311) diffraction rings for diamond are observed from the SAD patterns of UNCD/Si-NN_1 and UNCD/Si-NN_2

dx.doi.org/10.1021/am3016203 | ACS Appl. Mater. Interfaces 2012, 4, 5103−5108

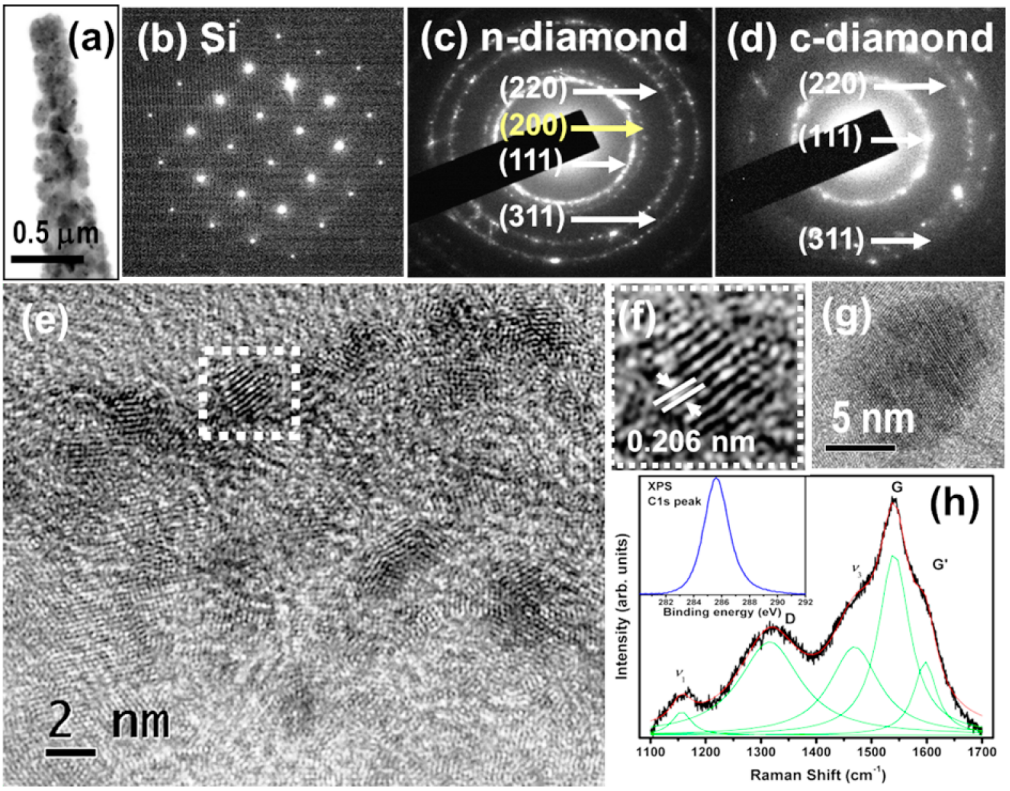

Figure 2. (a) Low-magnificationTEM image of low-temperature grown UNCD on a Si-NN after the UN_D process (UNCD/Si-NN_2), (b–d) SAD patterns of Si-NN, n-diamond, and c-diamond, respectively, (e) HRTEM image of 2 nm size c-diamond grains grown on a Si tip (UNCD/Si-NN_2) and (f) high-resolution image of a c-diamond grain with a lattice spacing of 0.206 nm (shown in the marked square region in e), (g) HRTEM image of a typical 5 nm diamond grain (UN_U process) and (h) Raman spectrum and XPS C1s peak (inset) of c-diamond grains (UNCD/Si-NN_2).

(Figure 1c, d). It is interesting to note that forbidden reflection rings corresponds to (200) of c-diamond is observed only for UNCD/Si-NN_1 (Figure 1c), which is an identification mark for n-diamond grains that exist usually with size of about 5-13 nm.[36−40] Such a SAD pattern is typically observed for the UNCD grown in CH_4/Ar medium, which has not gained much attention and their origin from energetic species has not been clearly explained yet.[10,13]

The UNCD/Si-NN_2 SAD pattern (Figure 2d) confirms that the grains are of cubic-diamond with Fd3m symmetry (c-diamond). The high resolution TEM image of UNCD/Si-NN_2 in Figure 2e shows the size of a UNCD grain is sub-2 nm and the size distribution is very uniform (1.85 nm). An enlarged structure image of marked square region in Figure 2e (Figure 2f) shows lattice spacing (d) of 0.206 nm, the typical d spacing of c-diamond.[36] For comparison, TEM image of UNCD grain size of about 5 nm (n-diamond) that typically grow in CH_4/Ar medium under the same growth conditions is shown in Figure 2g. In addition, although the sub-2 nm diamond grains prepared by the UN_D process are diamond structure with Fd3m symmetry (c-diamond), the 5 nm diamond grains prepared by the UN_U process are face-centered-cubic (fcc) structure with *Fm*3*m* symmetry (n-diamond), an allotropic form of diamond materials. A three-dimensional view of unit cells shows the difference of n-diamond and c-diamond structure (see Figure S3a, b in the Supporting Information). A two-dimentional view of the [220], [111], and [100] zone axes is also presented in Figure S3c, d in the Supporting Information to illustrate the difference in their atomic arrangement in a unit cell or in a typical grain.

The visible Raman spectrum (Figure 2h) and XPS carbon 1s core level (C1s) feature (inset in Figure 2h) of UNCD shown same behavior for the UNCD grown Si-NN after the different pre-nucleation processes. The Raman spectrum shows broadened peak at around 1330 cm^{-1} (D band) and at about 1540 cm^{-1} (G-band). A peak at around 1600 cm^{-1} (G′-band) is also observed, possibly from the nanocrystalline graphitic content in the sample.[41,42] There also exist peaks at around 1155 $cm^{-1}$and 1465 cm^{-1}, which are attributed to the ν_1 and ν_3 modes, respectively, of *trans*-polyacetylene (*trans*-PA) presented in the grain boundaries of UNCD films.[42] The XPS studies show that the binding energy is at 285.6 eV, which is the typical C1s peak position of diamond.[43]

The use of Si-NN can be advantageous over other Si-nanostructures, such as Si-nanowires (Si-NW), because its sharp apex with wide spacing can enhance the emission properties, since the electrical field screening effect can be circumvented and the field enhancement factor can be increased. Here we have investigated the EFE properties of the UNCD integrated Si-NN to explore their potential use in field emitter applications. Figure 3 shows the EFE properties of Si-NN before and after the nucleation processes and after UNCD growth. The inset shows Fowler-Nordheim (FN)[44] plots, $\ln(J/E^2)$ vs $1/E$ curves of the corresponding field emission data. The solid lines are the theoretical fitting using FN theory on the experimental data and the important EFE parameters extracted are given in Table S1 (Supporting Information). The turn-on field (E_0) is designated here as the applied field to achieve a current density of 1 μA. A schematic of the measurement method is also shown inside the Figure. The pristine Si-NN (Si-NN_0) shows a turn-on field of $(E_0)_{Si\text{-}NN0}$

dx.doi.org/10.1021/am3016203 | *ACS Appl. Mater. Interfaces* 2012, 4, 5103−5108

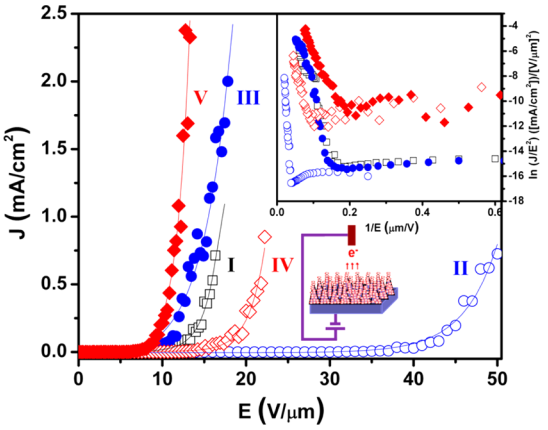

Figure 3. Field-emission properties of (I) pristine Si-NN, (II) Si-NN after the UN_U process, Si-NN_1, (III) UNCD/Si-NN_1, (IV) Si-NN after the UN_D process, Si-NN_2, and (V) UNCD/Si-NN_2. The insets show the FN plots of the corresponding field-emission data and schematic of the emission measurement method.

= 5.3 V/μm and current density of $(J_e)_{Si\text{-}NN0}$ = 0.4 mA/cm^2 at an applied field of 15 V/μm (curve I), whereas the UNCD/Si-NN_1 shows a turn-on field of $(E_0)_{Si\text{-}NN1}$ = 4.7 V/μm and current density of $(J_e)_{Si\text{-}NN1}$ = 1.0 mA/cm^2 at the same applied field (curve III). The UNCD coating has only moderately improved the EFE properties of Si-NN, which is unexpectedly contrary to the commonly observed phenomenon of pronounced enhancement of the EFE properties for UNCD coating on planar Si substrates. To understand the genuine factor that hinders the improvement on the EFE properties of UNCD/Si-NN_1, the EFE properties of UN_U-processed Si-NN_1 templates are examined. Curve II in Figure 3 shows that the turn-on field deleteriously increased to $(E_0)_{Si\text{-}NN1}$ = 26.0 V/μm with $(J_e)_{Si\text{-}NN1}$< 0.1 mA/cm^2 at the applied field of 15 V/μm. The degradation on the EFE properties of Si-NN_1 due to the UN_U process can be accounted for the changes in the morphology (cf. Figure 1a, b).

The field enhancement factor (β) of these Si-NN is estimated for understanding how the change in morphology alters their EFE properties. Because the theoretical calculation of β-value of UNCD nanoemitters from SEM micrograph is quite complex and is practically impossible, FN theory is used to approximately estimate this factor from EFE curves.[13,44] According to FN theory, $J = (A\beta^2E^2/\Phi)\exp(-B\Phi^{3/2}/E)$, where A and B are constants and Φ is the work function of the emitting material. By assuming the work function of Si-NN_0 to be the same as that of silicon materials (Φ_{Si} = 4.1 eV),[13] one can estimate the β-value of Si-NN_0 from the effective work function ($\Phi_{eff} = \Phi^{3/2}/\beta$), which is proportional to the slope of FN plot in the high-field segment. The results are $(\beta)_{Si\text{-}NN0}$ = 654 for pristine Si-NN and $(\beta)_{Si\text{-}NN1}$ = 128 for UN_U-processed Si-NN, inferring clearly that the degradation on the EFE properties due to the UN_U process for Si-NN results from the reduction in the field-enhancement factor for the emitting sites. The degradation on the characteristics of Si-NN templates can account for the cause of failure in improving the EFE properties for UNCD/Si-NN_1 emitters, even though UNCD coatings can usually improve the EFE properties of silicon materials.

The EFE studies on Si-NN_2 confirm the significant advantage of the UN_D process, where the highly deteriorating effect of the UN_U process on the Si-NN templates is effectively circumvented while keeping the high-aspect-ratio characteristic of the Si-NN structure. Curve IV in Figure 3 indicates that the EFE properties of Si-NN_2 can be turned on at $(E_0)_{Si\text{-}NN2}$ = 7.1 V/μm and attains $(J_e)_{Si\text{-}NN2}$ = 0.1 mA/cm^2 at the applied field of 15 V/μm. The β-value of Si-NN_2 is only slightly reduced to $(\beta)_{Si\text{-}NN2}$ = 581 due to the UN_D process. This value is comparable with $(\beta)_{Si\text{-}NN0}$ = 654 for the pristine Si-NN. Excellent enhancement in the EFE properties for UNCD/Si-NN_2 is also observed. Curve V in Figure 3 reveals that the EFE of UNCD/Si-NN_2 can be turned on at $(E_0)_{UNCD/Si\text{-}NN2}$ = 2.2 V/μm, attaining $(J_e)_{Si\text{-}NN2}$ = 2.4 mA/cm^2 at a low applied field of 13 V/μm. By assuming that the work function of nanocrystalline diamond prepared using CVD process is Φ_{dia} = 5.0 eV,[6] the β-value of UNCD coated Si-NN_2 is estimated as $\beta_{UNCD/Si\text{-}NN2}$ = 1491, which is very high as compared to $\beta_{UNCD/Si\text{-}NN1}$ = 810 for UNCD coated Si-NN_1. The turn-on field for UNCD/Si-NN_2 obtained in this work is comparable to other earlier reports[13,32,35] and the $\beta_{UNCD/Si\text{-}NN2}$-value obtained here is higher than that of the β-value reported for diamond grown silicon nanostructures.[13,32] The conformal coating capability of sub-2 nm grains in UNCD films is also possibly contributing largely for the improvement of the EFE properties. However, the superior field emitting characteristics of UNCD/Si-NN_2 can be mainly attributed to the large β-factor. Such a phenomenon in turn results from the large β-factor preserved for the Si-NN_2 in the UN_D process.

The salient feature of the UN_D ultrasonication process is that the grain size of UNCD film coated on Si-NN_2 is extremely small. The grain size of UNCD synthesized from energetic species after the UN_D process at nearly the same temperature (i.e., at 460 °C) is only about 2 nm in size, which is smaller than the UNCD grains ever reported in the literature (5−10 nm) that were grown on planar Si substrates.[11] It is still not clear how such an ultrasmall grains microstructure is resulted. The cross-sectional TEM image (Figure 1f) indicates that the UN_U process resulting in the formation of about 5 nm thick amorphous carbon layer at the interface between Si and UNCD. We have also noticed that the TEM sample preparation using ion milling process can cause detachment of UNCD film from Si substrate only for the samples undergone UN_U process (see Figure S4a in the Supporting Information). It indicates the thicker amorphous interlayer could make a weaker interface bonding between Si and UNCD for the UN_U-processed sample. Interestingly, the sample undergone UN_D process shows the interface layer of about 2 nm thick only (Figure 1g) and good adhesion of UNCD films to Si substrates (Figure S4b). The mechanism of diamond grains growth from these interface layers is not completely understood yet. The results signify that the interface layer thickness is possibly affecting the grain size of UNCD and the 2 nm interface region results in the formation of sub-2 nm c-diamond grains, whereas the 5 nm thick amorphous interface region results in the growth of 5 nm n-diamond grains through a solid−solid martensitic conversion.[36]

It is known that the pre-nucleation process creates defects as well as nucleation sites on substrate surface. During the pre-nucleation processes using mixed powder solution, the bombardments of nanodiamond and Ti particles creates defects and also react with the activated-Si surface to form Ti−Si or Si−C clusters. It should be noted that, the ultrasonication power induced cavitation effects for a substrate submerged to the bottom of a container might be different as compared to the one placed on top of the seeding solution. It is possible that the cavitation effects with larger particles at the bottom might also be contributing to the deteriorating effects than with smaller

dx.doi.org/10.1021/am3016203 | ACS Appl. Mater. Interfaces 2012, 4, 5103−5108

particles at the top of the solution. The finer the size of clusters, the lesser interface amorphous region formation and smaller the size of diamond nuclei, resulting in ultrasmall diamond grains for UNCD films. For the UN_U process, Si-NN_0 placed at the bottom of the container are subjecting to the bombardment of large Ti particles, which forms larger amorphous interface region, leading to larger-grains of UNCD films. The large UNCD grains form clusters and unevenly coat on Si-NN (cf. Figure 1b). In contrast, the mixtures floating on upper portion of the solution in the container usually contains very fine Ti powder (≤100 nm) and diamond particles are nano-size (4−20 nm). The Si-NN_0 placed at the top of the container are subjected to the bombardment of these fine particles, which possibly leads to the formation of ultrathin interface amorphous layer and hence results in extremely small grains for UNCD films. The UNCD layer coated on Si-NN_2 is not only more uniform in thickness, but also have more conformal covering on Si-NN, resulting in better contact with Si-NN. Both phenomena facilitate the electron transport from the Si to UNCD materials, further enhancing the EFE properties for the UNCD/Si-NN_2 emitters. Whether or not the difference in crystalline structure of UNCD influences the EFE properties of UNCD/Si-NN is not clear, which needs further investigation.

3. CONCLUSIONS

In summary, the conventional or UN_U process is not suitable to efficiently create the nucleation site on nanostructures and results in the formation of above 5 nm size n-diamond grains. Here, we have successfully developed a novel nucleation (UN_D) process to create the nucleation sites on nanostructures by without deteriorating its structure and properties. The UN_D process further helped the conformal growth of sub-2 nm UNCD grains (c-diamond) on the nanoneedles at low temperature and showed very high EFE performance. We expect that the realization of these allotropic forms of ultrananno size diamond materials from energetic species may find broad interest in developing nanosize diamond materials with controlled grain size and optimized properties by understanding their growth mechanism.

■ ASSOCIATED CONTENT

Ⓢ Supporting Information

Experimental details, Table S1 summarizing the EFE data of samples, schematics of the pre-nucleation techniques employed, FESEM and TEM images of the pre-nucleation materials, schematics of three-dimensional as well as two-dimensional view of unit cells and their typical arrangement for a single grain of c- and n-diamond, and low-magnification TEM cross-section images of the samples. This material is available free of charge via the Internet at http://pubs.acs.org.

■ AUTHOR INFORMATION

Corresponding Author

*E-mail: peetijoseph@gmail.com (J.P.T); inanlin@mail.tku.edu.tw (I.N.L).

Present Address

[§]WATLab and Department of Chemistry, University of Waterloo, Canada

Author Contributions

The manuscript was written through contributions of all authors. All authors have given approval to the final version of the manuscript.

Notes

The authors declare no competing financial interest.

■ ACKNOWLEDGMENTS

The authors thank the National Science Council (NSC 96-2112-M032-011-MY3) for financially supporting this study.

■ REFERENCES

(1) Fuchs, G. D.; Burkard, G.; Klimov, P. V.; Awschalom, D. D. *Nat. Phys.* **2011**, *7*, 789−793.
(2) Henderson, M. R.; Gibson, B. C.; Heidepriem, H. E.; Kuan, K.; Afshar, S. V.; Orwa, J. O.; Aharonovich, I.; Hanic, S. T.; Greentree, A. D.; Prawer, S.; Monro, T. M. *Adv. Mater.* **2011**, *23*, 2806−2810.
(3) Weimer, H.; Yao, N. Y.; Laumann, C. R.; Lukin, M. D. *Phys. Rev. Lett.* **2012**, *108*, No. 100501.
(4) Zhang, X. Q.; Lam, R.; Xu, X.; Chow, E. K.; Kim, H. J.; Ho, D. *Adv. Mater.* **2011**, *23*, 4770−4775.
(5) Schroder, T.; Schell, A. W.; Kewes, G.; Aichele, T.; Benson, O. *Nano Lett.* **2011**, *11*, 198−202.
(6) Zhu, W.; Kochanski, G. P.; Jin, S. *Science* **1998**, *282*, 1471−1473.
(7) Krauss, A. R.; Auciello, O.; Ding, M. Q.; Gruen, D. M.; Huang, Y.; Zhirnov, V. V.; Givargizov, E. I.; Breskin, A.; Chechen, R.; Shefer, E.; Konov, V.; Pimenov, S.; Karabutov, A.; Rakhimov, A.; Suetin, N. *J. Appl. Phys.* **2001**, *89*, 2958−2967.
(8) Joseph, P. T.; Tai, N. H.; Niu, H.; Lee, Y. C.; Lin, I. N. *J. Appl. Phys.* **2008**, *103*, No. 043720.
(9) Shang, N.; Papakonstantinou, P.; Wang, P.; Zakharov, A.; Palnitkar, U.; Lin, I. N.; Chu, M.; Stamboulis, A. *ACS Nano* **2009**, *3*, 1032−1038.
(10) Joseph, P. T.; Chen, H. C.; Tai, N. H.; Lin, I. N. *ACS Appl. Mater. Interfaces* **2011**, *3*, 4007−4013.
(11) Xiao, X.; Birrel, J.; Gerbi, J. E.; Auciello, O.; Carlisle, J. A. *J. Appl. Phys.* **2004**, *96*, 2232−2239.
(12) Joseph, P. T.; Tai, N. H.; Lin, I. N. *Appl. Phys. Lett.* **2010**, *97*, No. 042107.
(13) Tseng, Y. F.; Lee, Y. C.; Lee, C. Y.; Lin, I. N.; Chiu, H. T. *Appl. Phys. Lett.* **2007**, *91*, No. 063117.
(14) Goyal, V.; Subrina, S.; Nika, D. L.; Balandin, A. A. *Appl. Phys. Lett.* **2010**, *97*, No. 031904.
(15) Shamsa, M.; Ghosh, S.; Calizo, I.; Ralchenko, V.; Popovich, A.; Balandin, A. A. *J. Appl. Phys.* **2008**, *103*, No. 083538.
(16) Nika, D. L.; Pokatilov, E. P.; Balandin, A. A. *Appl. Phys. Lett.* **2008**, *93*, No. 173111.
(17) Goyal, V.; Sumant, A. V.; Teweldebrhan, D.; Balandin, A. A. *Adv. Funct. Mater.* **2012**, *22*, 1525−1530.
(18) Yu, J.; Liu, G.; Sumant, A. V.; Goyal, V.; Balandin, A. A. *Nano Lett.* **2012**, *12*, 1603−1608.
(19) Lee, S. T.; Peng, H. Y.; Zhou, X. T.; Wang, N.; Lee, C. S.; Bello, I.; Lifshitz, Y. *Science* **2000**, *287*, 104−106.
(20) Lee, H. J.; Jeon, H.; Lee, W. S. *J. Phys. Chem. C* **2012**, *116*, 9180−9188.
(21) Lifshitz, Y.; Meng, X. M.; Lee, S. T.; Akhveldiany, R.; Hoffman, A. *Phys. Rev. Lett.* **2004**, *93*, No. 056101.
(22) Chakk, Y.; Brener, R.; Hoffman, A. *Appl. Phys. Lett.* **1995**, *66*, 2819−2821.
(23) Tang, C.; Ingram, D. C. *J. App. Phys.* **1995**, *78*, 5745−5749.
(24) Liu, H.; Dandy, D. S. *Diamond Relat. Mater.* **1995**, *4*, 1173−1188.
(25) Anger, E.; Gicquel, A.; Wang, Z. Z.; Ravet, M. F. *Diamond Relat. Mater.* **2007**, *4*, 759−764.
(26) lhara, M.; Komiyama, H.; Okubo, T. *Appl. Phys. Lett.* **1994**, *65*, 1192−1194.
(27) Avigal, Y.; Hoffman, A. *Diamond Relat. Mater.* **1999**, *8*, 127−131.
(28) Chen, L. J.; Tai, N. H.; Lee, C. Y.; Lin, I. N. *J. Appl. Phys.* **2007**, *101*, No. 064308.
(29) Pradhan, D.; Lee, Y. C.; Lee, C. Y.; Tai, N. H.; Lin, I. N. *Diamond Relat. Mater.* **2006**, *15*, 1779−1783.

(30) Doicrycz, S. J.; Suslick, K. S. *Science* **1990**, *247*, 1067−1069.
(31) She, J. C.; Deng, S. Z.; Xu, N. S.; Yao, R. H.; Cheng, J. *Appl. Phys. Lett.* **2006**, *88*, No. 013112.
(32) McClain, D.; Solanki, R.; Dong, L.; Jiao, J. *J. Vac. Sci. Technol., B* **2006**, *24*, 20−24.
(33) Fonoberov, V. A.; Balandin, A. A. *Nano Lett.* **2006**, *6*, 2442−2446.
(34) Joseph, P. T.; Tai, N. H.; Chen, Y. F.; Lee, Y. C.; Cheng, H. F.; Lin, I. N. *Diam. Relat. Mater.* **2009**, *18*, 169−172.
(35) Tseng, Y. F.; Liu., K. H.; Lee, Y. C.; Lin, S. J.; Lin, I. N.; Lee, C. Y.; Chiu, H. T. *Nanotechnology* **2007**, *18*, No. 435703.
(36) Hirari, H.; Kondo, K. I. *Science* **1991**, *253*, 772−774.
(37) Prawer, S.; Peng, J. L.; Orwa, J. O.; McCallum, J. C.; Jamieson, D. N.; Bursill, L. A. *Phys. Rev. B (R)* **2000**, *62*, 360−363.
(38) Cowley, J. M.; Mani, R. C.; Sunkara, M. K.; O'Keeffe, M.; Bonneau, C. *Chem. Mater.* **2004**, *16*, 4905−4911.
(39) Peng, J. L.; Orwa, J. O.; Jiang, B.; PrawerS.; Bursill, L. A. *Int. J. Mod. Phys. B* **2001**, *15*, 3107−3123.
(40) Buljan, M.; Radovic, I. B.; Desnica, U. V.; Ivanda, M.; Jaksic, M.; Saguy, C.; Kalish, R.; Djerdj, I.; Tonejc, A.; Gamulin, O. *J. Appl. Phys.* **2008**, *104*, No. 034315.
(41) Mapelli, C.; Castiglioni, C.; Zerbi, G.; Mullen, K. *Phys. Rev. B* **1999**, *60*, 12710−12725.
(42) Ferrari, A. C.; Robertson, J. *Phys. Rev. B* **2001**, *63*, No.121405.
(43) Normand, F. L.; Hommet, J.; Szorenyi, T.; Fuchs, C.; Fogarassy, E. *Phys. Rev. B* **2001**, *64*, No. 235416.
(44) Fowler, R. H.; Nordheim, L. *Proc. R. Soc. London, Ser. A* **1928**, *119*, 173−181.